SCIENTIFIC BRIEFING
HYDROLOGICAL PROCESSES
Hydrol. Process. **23**, 1949–1959 (2009)
Published online 30 March 2009 in Wiley InterScience (www.interscience.wiley.com). DOI: 10.1002/hyp.7279

First-order exchange coefficient coupling for simulating surface water–groundwater interactions: parameter sensitivity and consistency with a physics-based approach

Brian A. Ebel,[1]*
Benjamin B. Mirus,[1]
Christopher S. Heppner,[2]
Joel E. VanderKwaak[3] and
Keith Loague[1]

[1] *Department of Geological and Environmental Sciences Stanford University, Stanford, CA 94305-2115*
[2] *Erler and Kalinowski, Inc., 1870 Ogden Drive, Burlingame, CA 94010*
[3] *Fusion Inc., Santa Clara, CA 95054*

*Correspondence to:
Brian A. Ebel, US Geological Survey, 345 Middlefield Rd., Menlo Park, CA.
E-mail: bebel32@stanford.edu

Abstract

Distributed hydrologic models capable of simulating fully-coupled surface water and groundwater flow are increasingly used to examine problems in the hydrologic sciences. Several techniques are currently available to couple the surface and subsurface; the two most frequently employed approaches are first-order exchange coefficients (a.k.a., the *surface conductance* method) and enforced continuity of pressure and flux at the surface-subsurface boundary condition. The effort reported here examines the parameter sensitivity of simulated hydrologic response for the first-order exchange coefficients at a well-characterized field site using the fully coupled Integrated Hydrology Model (*InHM*). This investigation demonstrates that the first-order exchange coefficients can be selected such that the simulated hydrologic response is insensitive to the parameter choice, while simulation time is considerably reduced. Alternatively, the ability to choose a first-order exchange coefficient that intentionally decouples the surface and subsurface facilitates concept-development simulations to examine real-world situations where the surface-subsurface exchange is impaired. While the parameters comprising the first-order exchange coefficient cannot be directly estimated or measured, the insensitivity of the simulated flow system to these parameters (when chosen appropriately) combined with the ability to mimic actual physical processes suggests that the first-order exchange coefficient approach can be consistent with a physics-based framework. Copyright © 2009 John Wiley & Sons, Ltd.

Key Words InHM; R5; runoff generation; coupling length; surface water-groundwater interaction; physics-based

Fully Coupled Flow Simulation Models: an Exciting Time in Hydrologic Modelling

The advent of hydrologic models capable of simulating fully coupled surface/subsurface water flow opens up many opportunities for interdisciplinary investigations in hydrologic sciences (Loague *et al.*, 2006). Table I lists selected hydrologic problems that have been examined using models that fully couple surface water and groundwater flow. There are many challenges for this fully coupled approach that are endemic to distributed physics-based models (Loague and VanderKwaak, 2004; Sudicky *et al.*, 2005; Qu and Duffy, 2007; Kollet and Maxwell, 2008a), such as scale issues (Blöschl and Sivapalan, 1995; Loague and Corwin, 2007; Wood *et al.*, 1988), initial conditions (Zehe and Blöschl, 2004; Noto *et al.*, 2008) and equifinality (Beven, 2006; Ebel and Loague, 2006). Beyond the aforementioned problems, there are conceptual and numerical issues specific to the fully coupled approach. Some of the numerical difficulties are being tackled in innovative ways such as adaptive timestep techniques (D'Haese *et al.*, 2007; Park *et al.*, 2008), advanced preconditioning methods (Ashby and Falgout, 1996; Herbst *et al.*, 2008), Newton–Krylov nonlinear solvers (Jones and Woodward, 2001; Knoll and Keyes, 2004; Hammond *et al.*, 2005) and parallel algorithms for solution (Kollet and Maxwell, 2006; Kollet and Maxwell, 2008a). One of the most significant conceptual obstacles is determining the most effective technique for coupling the surface and subsurface continua. While there are several coupling methods already in the literature (Morita and Yen, 2000, 2002; Fairbanks *et al.*, 2001; Discacciati *et al.*, 2002; Sulis *et al.*, 2006; Furman, 2008) and more on the

Received 9 September 2008
Accepted 12 January 2009

Table I. Selected hydrologic problems simulated using fully coupled surface water–groundwater models

Focus	References
Agricultural sustainability	Schoups *et al.* (2005)
Atmosphere–subsurface water and energy fluxes	Maxwell and Miller (2005), Maxwell *et al.* (2007), Kollet and Maxwell (2008a), Maxwell and Kollet (2008b)
Cumulative watershed effects	Carr (2006)
Dam removal	Heppner (2007), Heppner and Loague (2008)
Groundwater recharge	Lemieux *et al.* (2008), Markstrom *et al.* (2008), Smerdon *et al.* (2008)
Groundwater–lake interaction	Smerdon *et al.* (2007), Hunt *et al.* (2008)
Island scale erosion	Ran (2006)
New–old water/residence times	VanderKwaak (1999), VanderKwaak and Sudicky (2000), Jones *et al.* (2006), Cardenas (2008b), Cardenas *et al.* (2008), Kollet and Maxwell (2008b),
Pore-water pressure development and slope instability	Ebel (2007), Mirus *et al.* (2007), Ebel *et al.* (2007, 2008), BeVille (2007), Ebel and Loague (2008)
Radionuclide contamination/vulnerability	McLaren *et al.* (2000), Bixio *et al.* (2002)
Runoff generation	VanderKwaak and Loague (2001), Morita and Yen (2002), Loague *et al.* (2005), Kollet and Maxwell (2006), Heppner *et al.* (2007), Qu and Duffy (2007), Ebel *et al.* (2007, 2008), Jones *et al.* (2008), Li *et al.* (2008), Maxwell and Kollet (2008b), Mirus *et al.* (2009)
Sediment transport	Heppner *et al.* (2006), Heppner *et al.* (2007), Ran *et al.* (2007)
Solute transport	VanderKwaak (1999), VanderKwaak and Sudicky (2000), Ebel *et al.* (2007), Sudicky *et al.* (2008)
Stream-aquifer exchange	Weng *et al.* (2003), Gunduz and Aral (2003, 2005), Brookfield *et al.* (2008), Cardenas (2008a), Cardenas and Gooseff (2008), Peyrard *et al.* (2008)
Wetland-estuary exchange	Langevin *et al.* (2005)

way (Mario Putti, personal communication, 2008), two of the most common approaches are (i) first-order exchange coefficients (a.k.a., the *surface conductance* method) and (ii) forced continuity of pressure and flux at the surface–subsurface boundary condition. The purpose of this scientific briefing is to briefly examine these two coupling techniques and consider some of the weaknesses and merits of the first-order exchange coefficient approach.

Surface and Subsurface Flow

Subsurface flow

Variably saturated subsurface flow in porous media (without a separate preferential flow continua) can be expressed as:

$$f^{\mathrm{v}}\frac{\partial \phi S_{\mathrm{w}}}{\partial t} = \nabla \cdot f^{\mathrm{a}}\vec{q} \pm q^{\mathrm{b}} \pm q^{\mathrm{e}} \qquad (1)$$

where f^{v} is the volume fraction associated with each continuum (–), ϕ is porosity ($\mathrm{L^3\ L^{-3}}$), $\mathrm{S_w}$ is water saturation ($\mathrm{L^3\ L^{-3}}$), t is time (T), f^{a} is the area fraction associated with a given continuum (–), $\vec{q}$ is the Darcy flux ($\mathrm{LT^{-1}}$), q^b is a specified rate source/sink ($\mathrm{T^{-1}}$), and q^{e} is the rate of water exchange between the subsurface and surface continua (T^{-1}). Porous media compressibility is incorporated into ϕ as a function of ψ_{p} (Kropinski, 1990). The Darcy flux, $\vec{q}$, is given by:

$$\vec{q} = -k_{\mathrm{rw}}\frac{\rho_{\mathrm{w}} g}{\mu_{\mathrm{w}}}\vec{k}\nabla(\psi_{\mathrm{p}} + z) \qquad (2)$$

where k_{rw} is the relative permeability (–), ρ_{w} is the density of water ($\mathrm{ML^{-3}}$), g is the gravitational acceleration ($\mathrm{LT^{-2}}$), μ_{w} is the dynamic viscosity of water ($\mathrm{ML^{-1}\ T^{-1}}$), $\vec{k}$ is the permeability vector ($\mathrm{L^2}$), z is the elevation head (L), and ψ_{p} is the pressure head in the porous media (L).

Surface flow

Unsteady flow on the land surface can be represented using, for example, the diffusion-wave [alternatively known as the *zero inertia* or *noninertia* (Lighthill and Whitham, 1955; Yen and Tsai, 2001)] approximation of the depth-integrated shallow water equations describing conservation of mass:

$$\frac{\partial(S_{\mathrm{w_s}}\ h_{\mathrm{s}} + \psi_{\mathrm{s}}^{\mathrm{store}})}{\partial t} = \nabla \cdot \psi_{\mathrm{s}}^{\mathrm{mobile}}\vec{q}_{\mathrm{s}} \pm a_{\mathrm{s}} q^{b} \pm a_{\mathrm{s}} q^{\mathrm{e}} \qquad (3)$$

where $S_{\mathrm{w_s}}$ is the surface saturation (–), h_{s} is the average height of non-discretized surface microtopography (L), ψ_{s} is the depth of water (L) occurring as *mobile* or *stored* water, $\vec{q}_{\mathrm{s}}$ is the surface water velocity ($\mathrm{LT^{-1}}$), q^b is the source/sink rate (i.e. rainfall/evaporation) ($\mathrm{T^{-1}}$), q^{e} is the surface-subsurface water exchange rate ($\mathrm{T^{-1}}$), and a_{s} is the surface coupling length scale for surface/subsurface interaction (L). A two-dimensional (2D) Manning water depth/friction discharge equation allows estimation of surface water velocities:

$$\vec{q}_{\mathrm{s}} = -\frac{(\psi_{\mathrm{s}}^{\mathrm{mobile}})^{2/3}}{\vec{n}\,\Phi^{1/2}}\nabla(\psi_{\mathrm{s}} + z) \qquad (4)$$

where $\vec{n}$ is the Manning's surface roughness tensor ($\mathrm{TL^{-1/3}}$) and Φ is the friction (or energy) slope (–).

The diffusion-wave approximations are considered acceptable for channels under low-to-moderate velocity regimes (Hromadka *et al*, 1985) except in situations of

DOI: 10.1002/hyp

very steep waves (Todini and Bossi, 1987; Lamberti and Pilati, 1996). The omission of inertial terms has been shown to introduce errors on the order of 5–10% (Ahn *et al.*, 1993). Surface water flow can also be represented using other forms of the shallow water equations, such as the kinematic wave approximation used by Kollet and Maxwell (2006) or alternative approximations of the shallow water equations derived from the three-dimensional (3D) Navier–Stokes equations (Yeh *et al.*, 2005; Dawson, 2008).

First-Order Exchange Coefficient Coupling

As mentioned previously, the crux of the problem is how to specify the flux between the surface and subsurface continua (i.e. q^e in Equations (1) and (3)). Some fully coupled surface and subsurface flow models employ first-order exchange coefficients [e.g. Integrated Hydrology Model (*InHM*) (VanderKwaak, 1999), *MODHMS* (Panday and Huyakorn, 2004), *HydroGeoSphere* (Therrien *et al.*, 2005)]. First-order exchange coefficients have been used for some time to simulate subsurface flow with different coupled continua. For example, Barenblatt *et al.* (1960) and Warren and Root (1963) coupled fracture and porous media continua using first-order exchange coefficients driven by gradients in pressure between the two continua. Numerous authors have demonstrated the utility of the first-order exchange coefficients between macropore or fracture continua with a soil/rock matrix (van Genuchten and Wierenga, 1976; van Genuchten and Dalton, 1986; Sudicky, 1990; Jarvis *et al.*, 1991; Gerke and van Genuchten, 1993a, b; Gerke and van Genuchten, 1996; Therrien and Sudicky, 1996). The first-order exchange coefficient approach has also been employed successfully by, for example, Bencala (1983, 1984) and Bencala *et al.* (1984), to examine hyporheic zone flow. An example of an approximation used to specify q^e is provided by VanderKwaak (1999) as:

$$q^e_{sp} = \alpha^e_{sp}(\psi_s - \psi_p) = -q^e_{ps} \tag{5}$$

where the sp and ps subscripts denote surface to porous media and porous media to surface exchange, respectively. The first-order exchange coefficient, α^e_{sp} ($L^{-1}\ T^{-1}$), can be approximated using (VanderKwaak, 1999):

$$\alpha^e_{sp} = k^e_{rw}\varphi^e_{sp}\frac{\zeta^e_s}{a_s} \tag{6}$$

where k^e_{rw} is the relative permeability of the exchange interface relative to water (−), ζ^e_s is the surface exchange interface area to volume ratio ($L^2\ L^{-3}$), and φ^e_{sp} is analogous to an interface exchange rate ($L\ T^{-1}$), which can be approximated as VanderKwaak (1999):

$$\varphi^e_{sp} = \chi^e\frac{\rho_w g}{\mu_w} f^{a\ zz}_p k^{zz}_p \tag{7}$$

where χ^e is a dimensionless exchange scaling coefficient (−), $f^{a\ zz}_p$ is the isotropic porous media area fraction in the *z* direction (−), and k^{zz}_p is the isotropic porous media permeability in the *z* direction (L^2).

There are a number of parameters in Equations (6–7) for which no accepted measurement or objective estimation exists. There have been efforts to represent the surface coupling length scale as a characteristic length scale for momentum exchange between the surface and subsurface continua related to the permeability of the porous media (Richardson and Parr, 1991; VanderKwaak, 1999):

$$a_s \propto \sqrt{k_p} \tag{8}$$

The dimensionless exchange scaling coefficient, χ^e, has also been suggested as a method to reduce the interface relative permeability to account for soil crusts and seals or to eliminate surface–subsurface exchange entirely by setting χ^e to zero (VanderKwaak, 1999). In light of the inability to measure the parameters that comprise the first-order exchange coefficient (e.g. the surface coupling length scale), it has been considered as a lumped conceptual fitting parameter by Bencala (1984). It should be noted that the first-order exchange coefficient principle is also used, in a modified form, to couple solute transport between surface and subsurface continua (VanderKwaak, 1999).

Currently, the inability to directly estimate the parameters that control the surface–subsurface exchange in the first-order exchange coefficient method has made universal application of the concept problematic in certain situations of surface water and groundwater interaction. It should be pointed out that the exchange coefficient approach used by VanderKwaak (1999) was taken from the subsurface preferential flow literature, where the coupling length scale is typically small (i.e. 10^{-4} m). The exchange coefficient technique may work poorly for large surface coupling length scales that cause a small first-order exchange coefficient (Equation (6)), which result in a physically unrealistic disequilibrium in pressure between the surface and subsurface (Equation (5)). This problem was observed by Kollet and Zlontik (2003) in a coupled surface water–ground water setting in a fluvial system where the interface lengths were on the order of metres and likely to be highly spatially variable to account for heterogeneous sediments and bedform geometry.

Enforced Continuity of Pressure between the Subsurface and Surface Continua

Enforcing simultaneous continuity of pressure between the surface and subsurface, typically accomplished implicitly using iterative boundary condition matching, is an alternative to the first-order exchange coefficient approach, predating it by decades (Smith and Woolhiser, 1971; Freeze, 1972a, b; Akan and Yen, 1981; Smith and Hebbert, 1983; Abbott *et al*, 1986a, b; Perkins and Koussis, 1996; Refsgaard and Storm, 1996; Bronstert and Plate, 1997). Brown (1995) presents an example of

Hydrol. Process. **23**, 1949–1959 (2009)
DOI: 10.1002/hyp

enforcing simultaneous pressure continuity without iterative boundary condition matching. Dawson (2006, 2008) and Furman (2008) review other methods and efforts that employ pressure continuity at boundary conditions.

Recent work by Kollet and Maxwell (2006), Maxwell *et al*. (2007), Kollet and Maxwell (2008a) and Maxwell and Kollet (2008a) has enforced continuity of flux and fluid pressure between the surface and subsurface continua and overcome the obstacles encountered by previous researchers, including using an innovative parallelized computing approach. Other efforts have also successfully implemented the direct continuity coupling approach. For example, Yeh *et al*. (2005) coupled the one-dimensional (1D) St Venant equations describing channel flow and the 2D St. Venant equations describing overland flow (with both the channel and overland-flow regimes allowing flexible use of either the kinematic, diffusive and fully dynamic wave forms) coupled to a 3D representation of variably saturated subsurface flow employing Richards equation for both unsaturated and saturated zones. Dawson (2008) also uses direct continuity of flux and pressure across the surface–subsurface interface, with surface flow represented using the 2D shallow water equations, including inertial effects, coupled to 3D variably saturated flow estimated using Richards equation.

An example of coupling via pressure and flux continuity is presented by Dawson (2008), where continuity of pressure is implemented as a time-dependent prescribed head (Dirichlet type) as the boundary condition at the surface–porous media interface, with $\psi_s = \psi_p$ (assuming hydrostatic pressures in the surface continua) and continuity of flux between the surface and subsurface continua is introduced as a source/sink term in the surface equations. Other similar approaches include those used by Yeh *et al*. (2005) and Kollet and Maxwell (2006). More complex approaches to dealing with the exchange and boundary conditions between free surface flow and porous media flow are presented in Salinger *et al*. (1994), Gartling *et al*. (1996) and discussed in Dawson (2008), and references therein.

Differences between the First-Order Exchange Coefficient Approach and the Enforced Continuity Approach

Inspection of Equations (3) and (5) reveals that a modeller could make the informed decision that the hydrologic system being simulated has a *tightly coupled* surface and subsurface and use a large exchange coefficient (e.g. with a small surface coupling length scale). This will tend to promote continuity between the surface and subsurface and make the first-order exchange coupling coefficient approach approximately the same as enforcing contemporaneous continuity of pressure and flux via boundary conditions and source/sink terms. The following sections examine the sensitivity of simulated hydrologic response to the value of the surface coupling length scale and explore reasons why the first-order exchange coefficient approach may be useful in a conceptual framework.

Sensitivity of Simulated Hydrologic Response to the First-Order Exchange Coefficient: Effects of the Surface Coupling Length Scale

In this study, we vary the surface coupling length scale parameter, a_s, to examine the sensitivity of simulated hydrologic response to the first-order exchange coefficient at the well studied R-5 catchment (VanderKwaak and Loague, 2001; Loague and VanderKwaak, 2002). R-5 is located near Chickasha, Oklahoma, within the Washita River Experimental Watershed. Figure 1 shows the topography and near-surface permeability at the 0·1 km^2 catchment, which consists of rolling prairie grassland that was subjected to continuous well-managed grazing for decades. As reported by VanderKwaak and Loague (2001) and Heppner *et al*. (2007), a fair amount of data was collected for R-5 over a period of 30 years. The integrated and distributed hydrologic observations at R-5 have fuelled numerous simulation efforts for the site. The early simulation efforts (with a quasi-physically based Horton type model) include the work by Loague and Freeze (1985), Loague (1990) and Loague and Kyriakidis (1997). More recent simulations at R-5 have addressed the importance of both the Horton (i.e. infiltration excess) and Dunne (i.e. saturation excess) runoff generation mechanisms and used simulated runoff to drive sediment transport modelling (VanderKwaak and Loague, 2001; Loague *et al*., 2005; Heppner *et al*., 2007). R-5 event number 68 (Loague, 1990) has been carefully analysed in these more recent process-based simulation efforts, and is employed here to examine the sensitivity of simulated hydrologic response (both integrated and distributed) to the surface coupling length scale in the fully coupled surface water–groundwater model *InHM* (VanderKwaak, 1999). Four different surface coupling length scales (i.e. 10^{-5}, 10^{-4}, 10^{-2}, 10^{-1} m) are used here to examine the sensitivity of the integrated response at the weir (Figure 1) and the distributed response at a channel and a hillslope location (Figure 1).

The setup of the R-5 boundary-value problem (BVP), and subsequently the simulation results reported here, is most closely related to that of Heppner *et al*. (2007). The only differences between the BVP from Heppner *et al*. (2007) and the one used in this work are that the depression storage and height of microtopography are both set to 0·0005 m and the hydraulic property variations associated with the roads and remnant buffalo wallows are removed. The topography in the finite-element mesh associated with the road and the remnant wallows is still included in the BVP used here. The initial conditions for event 68 are gleaned from the long-term 8-year duration simulations by Heppner *et al*. (2007). It should be pointed out that Heppner *et al*. (2007) used a surface coupling length scale of 10^{-2} m. The finite element mesh for the surface contains 1603 nodes and 3095 elements and for the subsurface contains 62 517 nodes and 117 610

Hydrol. Process. **23**, 1949–1959 (2009)
DOI: 10.1002/hyp

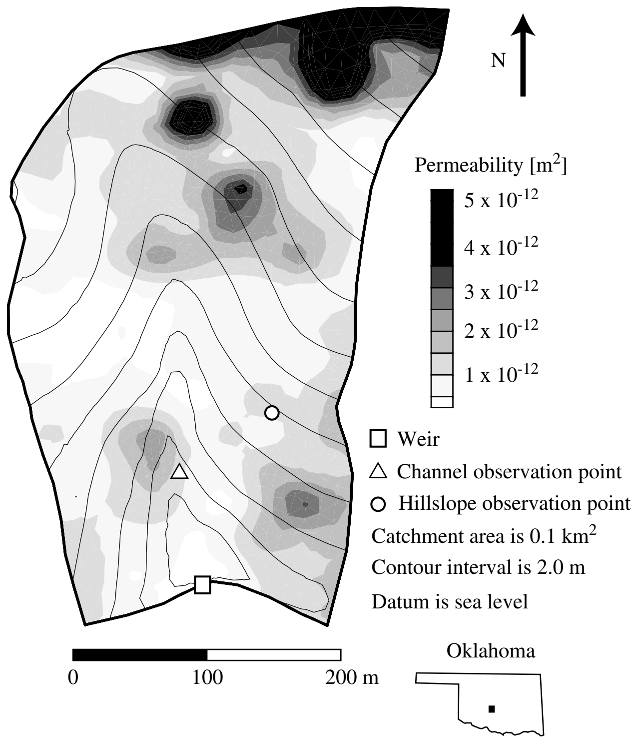

Figure 1. Map of the R-5 catchment in Oklahoma, showing spatial variations in both topography and permeability (after Heppner *et al.*, 2007). The simulated observation locations for the discharge (weir) and pressure heads (hillslope and channel) shown in Figures 2–4 are marked

elements. The vertical nodal discretization varies from 0·05 to 0·25 m and the horizontal nodal discretization varies from 1 to 20 m.

Figure 2 presents the event 68 hyetograph and simulated discharge hydrographs for four different coupling length scenarios. The times denoted as T_R and T_Q in Figure 2 are the times of the peak rainfall rate and the peak simulated discharge (for the 10^{-2} m surface coupling length scale), respectively. The simulated discharge hydrographs for the 10^{-5}, 10^{-4} and 10^{-2} m surface coupling length scales are imperceptibly different, while the 10^{-1} m surface coupling length scale shows a deviation at early times and less runoff at T_Q. The 10^{-1} m length scale decouples the surface and subsurface continua enough to reduce infiltration, which correspondingly results in additional runoff generation by the Horton mechanism near T_R. The reduced infiltration at early times decreases the runoff contribution from the Dunne mechanism at later times near T_Q. Figure 2 shows that at surface coupling length scales greater than 10^{-2} m, the simulated integrated response is affected in terms of timing and magnitude by controlling surface–subsurface water exchange. It should be noted that the cumulative discharge for the 10^{-1} m coupling length simulation is 47·7 m^3 greater (or 0·0005 m in terms of total runoff depth) relative to the 10^{-2} m simulation. While the implications for event-scale simulations may be minor, the effect of surface coupling length scale choice at the threshold where the simulated integrated response is affected could have significant impacts on the long-term (i.e. annual scale) simulated water balance and surface/subsurface water partitioning.

Figure 3 shows the simulated surface (ψ_S) and subsurface (ψ_P) pressure heads at the hillslope (Figure 3a) and channel (Figure 3b) observation points for the 10^{-2} m surface coupling length scale simulation. The surface and porous media-simulated observation points are nodes in the finite-element mesh that are co-located in space but separated, in theory, by the coupling layer. The difference in pressure head between these two essentially co-located points in separate continua is representative of the discontinuity in pressure between the two continua resulting from the coupling technique. The surface pressure head is the surface water depth and obviously cannot decrease below zero. It makes sense, therefore, that when surface water depth equals zero, that ψ_S and ψ_P can be quite different, irrespective of the surface coupling length scale. Inspection of Figure 3 when ψ_S is greater than zero demonstrates that the 10^{-2} m surface coupling length scale enforces near-continuity of pressure between the surface and subsurface continua, with only a couple of millimetres difference. This small difference is, in part, the result of the near-surface relative permeability averaging for the porous media continuum.

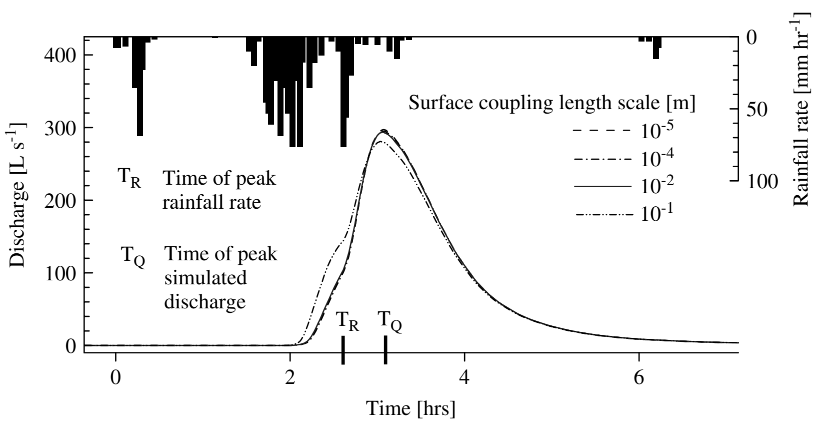

Figure 2. Simulated discharges and observed hyetograph for R-5 rainfall event number 68 (Loague, 1990) for four different surface coupling length scales. T_R and T_Q are the times of the peak rainfall rate and the peak simulated discharge, respectively. The time of peak simulated discharge (T_Q) is based on the simulation using a 10^{-2} m surface coupling length scale

DOI: 10.1002/hyp

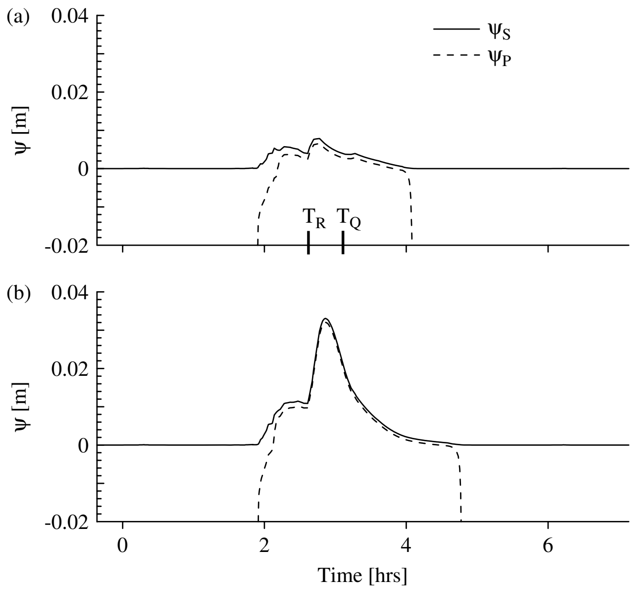

Figure 3. Simulated surface (ψ_S) and subsurface (ψ_P) pressure head values at the observation points shown in Figure 1 for R-5 event number 68 (Figure 2) for the 10^{-2} m surface coupling length scale used by Heppner *et al.* (2007). (a) Hillslope-simulated observation point, (b) channel-simulated observation point

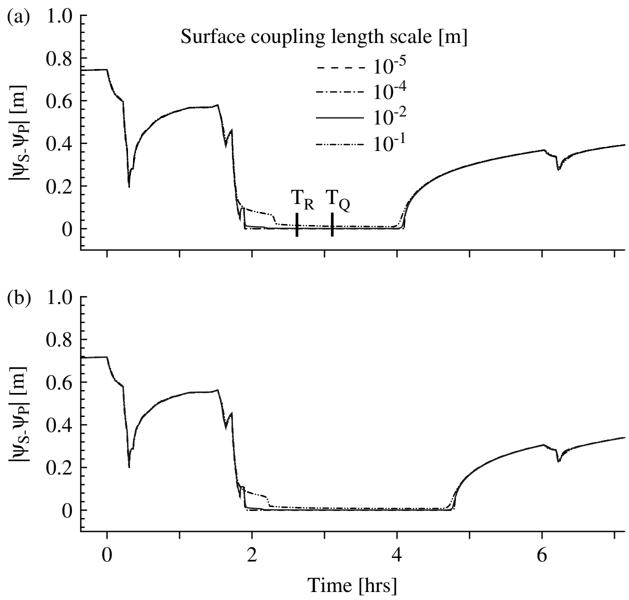

Figure 4. Absolute value of the differences between simulated surface (ψ_S) and subsurface (ψ_P) pressure heads for four different surface coupling length scales at the observation points shown in Figure 1 for R-5 event number 68 (Figure 2). (a) Hillslope-simulated observation point, (b) channel-simulated observation point

Figure 4 examines the threshold in surface coupling length scale that causes near-continuity of pressure between the continua to break down. In Figure 4, the absolute value of the difference in pressure head (i.e. $|\psi_S - \psi_P|$) is shown for the hillslope (Figure 4a) and channel (Figure 4b)-simulated observation points for the four different surface coupling length scale scenarios. For Figure 4a and b, as with Figure 3, the absolute differences are large when surface water depth (ψ_S) is zero and non-meaningful for the discussion presented here. Examination of the time period when simulated ψ_S is greater than zero illustrates the minimal sensitivity of the surface–subsurface pressure discontinuity to the surface coupling length scale choice for 10^{-5}, 10^{-4} and 10^{-2} m. Close inspection of Figure 4a and b reveals two periods, at the beginning and end of overland flow (at approximately 2 and 5 h), that show slight differences in surface–subsurface pressure discontinuity for the 10^{-2} m coupling length relative to the 10^{-5} and 10^{-4} m simulations for both the hillslope and channel points. The surface–subsurface pressure discontinuity for the 10^{-1} m coupling length simulation shows substantial deviation from the 10^{-5}, 10^{-4} and 10^{-2} m simulations at the initiation and cessation of runoff generation. Figure 4a and b also shows that for the entire duration of surface ponding, the 10^{-1} m coupling length facilitates constant disequilibrium between the surface and subsurface continua in the channel and on the hillslope.

Figure 5 presents snapshots of simulated pressure heads (i.e. ψ_S, ψ_P) and absolute pressure head differences (i.e. $|\psi_S - \psi_P|$) at T_R and T_Q for the four different surface coupling length scale scenarios. Inspection of the ψ_S snapshots at T_R shows indistinguishable/minor differences between the different coupling length simulations with the exception of the 10^{-1} m coupling length. The ψ_S snapshot at T_R for the 10^{-1} m coupling length reveals slightly smaller surface water depths on the hillslopes, but deeper surface water depths in the channel and in the weir pond, which is the result of the larger Horton runoff contribution earlier in the event for the 10^{-1} m coupling length simulation relative to the other three scenarios (Figure 2). The ψ_P snapshots at T_R show no difference between the 10^{-5} and 10^{-4} m coupling length simulations, some minor differences between the $10^{-5}/10^{-4}$ m and 10^{-2} m simulations, and large differences between the smaller coupling length simulations and the 10^{-1} m coupling length. These ψ_P differences are controlled by the near-surface permeability (Figure 1), with lower permeability enhancing disequilibrium between the surface and subsurface continua, which is not surprising given the direct proportionality between porous media permeability (k_p) and the surface–subsurface exchange flux shown in Equation (7).

The dependence of surface–subsurface disequilibrium on the porous media permeability is expressed in Figure 5 by the $|\psi_S - \psi_P|$ snapshots at T_R and T_Q. The $|\psi_S - \psi_P|$ snapshots at T_R in Figure 5 show that there is no perceptible difference in pressure between the surface and subsurface continua, irrespective of subsurface permeability for the 10^{-5} and 10^{-4} m coupling length simulations. The effect of the subsurface permeability begins to show up in the $|\psi_S - \psi_P|$ snapshot at T_R for the 10^{-2} m coupling length, and is fully evident in the low-permeability areas for the $|\psi_S - \psi_P|$ snapshots at T_R for the 10^{-1} m coupling length where the lower permeability reduces the surface–subsurface exchange (i.e. infiltration), resulting in an unsaturated near-surface porous media continuum. The same trends are visible in the $|\psi_S - \psi_P|$ snapshots

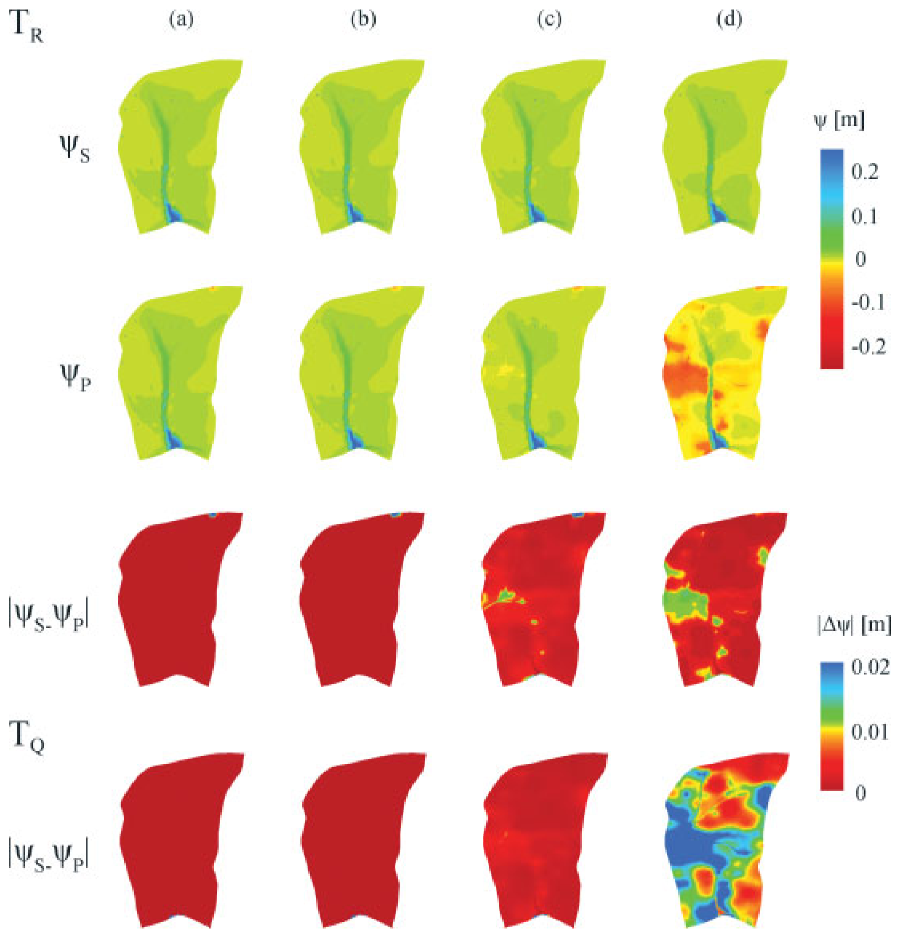

Figure 5. (T_R) Snapshots in time of simulated surface (ψ_S) and subsurface (ψ_P) pressure head values and the absolute value of the difference $|\psi_S - \psi_P|$ between the surface/subsurface values at the time of peak rainfall rate for R-5 event number 68 (Figure 2) for four different surface coupling length scales. (a) 10^{-5} m, (b). 10^{-4} m, (c) 10^{-2} m, (d) 10^{-1} m. (T_Q) Snapshots in time of the absolute value of the difference $|\psi_S - \psi_P|$ between the surface/subsurface values at the time of peak-simulated discharge for R-5 event number 68 (Figure 2) for the same four coupling lengths

at T_Q, with only the 10^{-1} m coupling length simulation showing substantial surface–subsurface disequilibrium. The permeability control on surface–subsurface discontinuity is clear in the $|\psi_S - \psi_P|$ snapshot at T_Q for the 10^{-1} m coupling length, with the low permeability areas (Figure 1) exhibiting substantial absolute differences (note, the absolute difference are exaggerated owing to the unsaturated porous media continuum).

The simulation results shown here illustrate that the integrated and distributed hydrologic response is insensitive to the surface coupling length scale, provided a reasonable value is chosen. For R-5 rainfall-runoff event 68 (Loague, 1990), the 10^{-1} m coupling length caused perceptible changes in the simulated discharge, subsurface pressure heads and the dynamics of runoff generation between the interacting Horton and Dunne mechanisms (Figure 2) by changing the infiltration capacity via reduced surface–subsurface coupling. It appears, based on the event 68 simulations reported here, that 10^{-2} m [i.e. the value used by Heppner *et al.* (2007)] is the threshold coupling length for not detrimentally impacting the R-5 simulation results. The surface coupling length scale that preserves near-continuity of pressure between the surface and subsurface likely depends on topography, mesh discretization, hydraulic properties (e.g. permeability, characteristic curves), surface properties (e.g. Mannings roughness, mobile water depths, microtopography) and dominant runoff generation mechanisms. Therefore, some care should be exercised before applying the surface coupling length threshold reported here to another site without sufficient testing.

First-Order Exchange Coefficients

One may ask why not set the surface coupling length to a very small value like 10^{-10} m, which greatly increases the first-order exchange coefficient, and enforce surface–subsurface near-continuity? The answer is simulation time; the disparate timescales between surface and subsurface hydrologic response presents problems for numerical solution of the governing partial differential equations (Beven, 1985) and is one of the principal reason why the first-order exchange coefficient approach was pursued for surface–subsurface coupling. The first-order exchange coefficient coupling contributes additional nonlinear terms in the model used in this study (i.e. *InHM*), similar to an external boundary condition. These terms tend to zero when they are least hydrologically important (i.e. when there is no surface–subsurface exchange, and the surface and subsurface domains are effectively decoupled); similarly, larger coupling length scales decrease the magnitude of the coupling terms by a constant factor. In either case, the coupled system of equations becomes easier to solve. For example, for the R-5 rainfall-runoff event considered here, the 10^{-5}, 10^{-4}, 10^{-2} and 10^{-1} m coupling length simulations took 5·0, 3·5, 2·0 and 2·0 h of computer time. There is a clear advantage of using the 10^{-2} m coupling length over the 10^{-5} and 10^{-4} m coupling lengths, in terms of simulation time, while still preserving the physics of simulated hydrologic response (in contrast to the 10^{-1} m value). There is also no gain in terms of simulation time going from the 10^{-2} to the 10^{-1} m coupling length. Finding the *sweet spot* in coupling length (i.e. first-order exchange coefficient) that minimizes simulation cost in terms of time, while not substantially altering the simulated response, would be critical for a long-duration (i.e. many years) simulation.

Beyond gains in simulation time, choosing a larger coupling length (e.g. 10^{-1} m at R-5) allows mimicry of physical and chemical processes that cause disequilibrium between the surface and subsurface continua, even if we cannot precisely represent the underlying mechanisms. This would not be the first time in hydrology that conceptual possibilities have outpaced measurement; for example, Philip (1957) formulated sorptivity before Talsma (1969) measured it. Interestingly enough, recent research has shown that micro-scale sorptivity may lead to surface–subsurface hydrologic disequilibrium (Hallett *et al*., 2004). There are many physical and chemical processes that may lead to a hydrologic disconnect between the surface and subsurface such as (i) agricultural cultivation (Bajracharya and Lal, 1999; Robinson and Phillips, 2001), (ii) manure application (Roberts and Clanton, 2000), (iii) fire effects (Mills and Feya, 2004), (iv) artificial recharge and wastewater application (Behnke, 1969; Siegrist, 1987) and (v) structural surface sealing by raindrop impacts and sudden wetting (Mualem *et al*., 1990; Römkens *et al*., 1990; Bresson and Cadot, 1992; Assouline, 2004). Many of these processes impact infiltration by reducing interface permeability and could also be mimicked by decreasing the dimensionless exchange scaling coefficient, χ^e, in Equation (7), which decreases the first-order exchange coefficient (VanderKwaak, 1999). A modeller could develop hypotheses and guide field investigations of the aforementioned processes by employing a small first-order exchange coefficient to simulate disequilibrium between the surface and subsurface. It should be pointed out that one could also mimic disequilibrium between surface water and groundwater flow regimes in the enforced continuity of flux and pressure coupling approach by choosing appropriate parameters.

To the best of the authors' knowledge, there is no way to measure some of the parameters that comprise the first-order exchange coefficient, which gives rise to the argument that this approach has no place in a model that purports to be *physics-based*. Of course, the first-order exchange coefficient can be viewed as another lumped conceptual parameter, which only further enhances the already daunting problem of equifinality, especially with respect to simulating the integrated hydrologic response (discharge) without considering the distributed hydrologic response model performance (Ebel and Loague, 2006). However, we have shown here that the first-order exchange coefficient can be set to a reasonable value which enforces near-continuity in pressure between the surface and subsurface. The ability to minimize the influence of the first-order coupling coefficient allows the underlying physics-based nature of the model to be preserved. At the same time, the first-order exchange coefficient approach offers useful flexibility that allows the modeller to control the degree of decoupling between surface water and groundwater flow, preserving tight coupling when desired or loose coupling for investigative purposes.

Summary

This *scientific briefing* focuses on the importance and principal methods of coupled simulation of surface water and groundwater interaction, focusing on the first-order exchange coefficient approach. We have shown here, for a well-studied field example, that the surface coupling length scale can be chosen to maximize computational efficiency, while maintaining realism of physical process representation. It is our opinion that all the methods currently available in the scientific literature for surface–subsurface flow coupling have merit for certain situations and none of them has been thoroughly demonstrated to be superior. The current approaches are likely to be the *tip of the iceberg* and a great deal of interesting theoretical and applied research on methods for coupling surface and subsurface flow is likely forthcoming in the next few decades. We look forward to the next generation of numerical models and, hopefully, the equally rigorous field experiments designed to examine the conceptual foundation and performance of these models.

Acknowledgements

This work was supported by National Science Foundation grants EAR-0409133 and EAR-0438749. The ideas presented here benefitted from discussions with Adrianne Carr, Qihua Ran, and Mario Putti.

References

Abbott MB, Bathurst JC, Cunge JA, O'Connell PE, Rasmussen J. 1986a. An introduction to the European Hydrological System-Systèm Hydrologique Européen, "SHE", 1: history and philosophy of a physically-based, distributed modeling system. *Journal of Hydrology* **87**: 45–59.

Abbott MB, Bathurst JC, Cunge JA, O'Connell PE, Rasmussen J. 1986b. An introduction to the European Hydrological System-Systèm Hydrologique Européen, "SHE", 2: structure of a physically-based, distributed modeling system. *Journal of Hydrology* **87**: 61–77.

Ahn S, Kim G, Choi G. 1993. On the applicable ranges of kinematic and diffusion models in open channels. *In Hydraulic Engineering '93, ASCE Proceedings of Specialty Conferences*, San Francisco.

Akan AO, Yen BC. 1981. Mathematical model of shallow water flow over porous media. *Journal of Hydraulics Division* **ASCE H14**: 479–494.

Ashby SF, Falgout RD. 1996. A parallel multigrid preconditioned conjugate gradient algorithm for groundwater flow simulations. *Nuclear Science and Engineering* **124**: 145–159.

Assouline S. 2004. Rainfall-induced soil surface sealing: a critical review of observations, conceptual models, and solutions. *Vadose Zone Journal* **3**: 570–591.

Bajracharya RM, Lal R. 1999. Land use effects on soil crusting and hydraulic response of surface crusts on a tropical Alfisol. *Hydrological Processes* **13**: 59–72.

Barenblatt GI, Zheltov IP, Kochina IH. 1960. Basic concepts in the theory of homogenous seepage in fissured rocks. *Journal of Applied Mathematics and Mechanics* **24**: 1286–1303.

Behnke JJ. 1969. Clogging in surface spreading operations for artificial ground-water recharge. *Water Resources Research* **5**: 870–876.

Bencala KE. 1983. Simulation of solute transport in a mountain pool-and-riffle stream with a kinetic mass transfer model. *Water Resources Research* **19**: 732–738.

Bencala KE. 1984. Interactions of solutes and streambed sediment 2. A dynamic analysis of coupled hydrologic and chemical processes that determine solute transport. *Water Resources Research* **20**: 1804–1814.

Bencala KE, Kennedy VC, Zellweger GW, Jackman AP, Avazino RJ. 1984. Interactions of solutes and streambed sediment 1. An experimental analysis of cation and anion transport in a mountain stream. *Water Resources Research* **20**: 1797–1803.

Beven KJ. 1985. Distributed models. In *Hydrologic Forecasting*, Anderson MG, Burt TP (eds). John Wiley and Sons: New York; 405–435.

Beven K. 2006. A manifesto for the equifinality thesis. *Journal of Hydrology* **320**: 18–36.

BeVille SH. 2007. *Physics-based simulation of near-surface hydrologic response for the Lerida Court landslide in Portola Valley, California*, MS Thesis, Stanford University, Stanford.

Bixio A, Gambolati G, Paniconi C, Putti M, Shestopalov V, Bublias V, Bohuslavsky A, Kasteltseva N, Rudenko Y. 2002. Modeling groundwater-surface water interactions including effects of morphogenetic depressions in the Chernobyl exclusion zone. *Environmental Geology* **42**: 162–177.

Blöschl G, Sivapalan M. 1995. Scale issues in hydrological modelling: a review. *Hydrological Processes* **9**: 251–290. DOI:10·1002/hyp.3360090305.

Bresson LM, Cadot L. 1992. Illuviation and structural crust formation on loamy temperate soils. *Soil Science Society of America journal* **56**: 1565–1570.

Bronstert A, Plate EJ. 1997. Modelling of runoff generation and soil dynamics for hillslopes and microcatchments. *Journal of Hydrology* **189**: 177–195.

Brookfield AE, Sudicky EA, Park Y-J. 2008. *Analysis of Thermal Stream Loadings In A Fully-Integrated Surface/Subsurface Modelling Framework*, vol. **321,** *IAHS-AISH Publication*; 117–123.

Brown DL. 1995. *An analysis of transient flow in upland watersheds: interactions between structure and process*. Ph.D. Dissertation, Department of Soil Science, University of California, Berkeley, 225.

Cardenas MB. 2008a. The effect of river bend morphology on flow and timescales of surface water-groundwater exchange across pointbars. *Journal of Hydrology* **362**: 134–141. DOI:10·1016/j.jhydrol.2008·08·018.

Cardenas MB. 2008b. Surface-ground water interface geomorphology leads to scaling of residence times. *Geophysical Research Letters* **35**: L08402. DOI:10·1029/2008GL033753.

Cardenas MB, Gooseff MN. 2008. Comparison of hyporheic flow under uncovered and covered channels based on linked surface-ground-water simulations. *Water Resources Research* **44**: W03418, DOI:10·1029/2007WR006506.

Cardenas MB, Wilson JL, Haggerty R. 2008. Residence time of bedform-driven hyporheic exchange. *Advances in Water Resources* **31**: 1382–1386, DOI:10·1016/j.advwatres.2008·07·006, 2008.

Carr AE. 2006. *Physics-based simulations of hydrologic response and cumulative watershed effects*. PhD Dissertation, Department of Geological and Environmental Sciences, Stanford University, Stanford.

Dawson C. 2006. Analysis of discontinuous finite element methods for ground water/surface water coupling. *SIAM Journal on Numerical Analysis* **44**: 1375–1404, DOI:10·1137/050639405.

Dawson C. 2008. A continuous/discontinuous Galerkin framework for modeling coupled subsurface and surface water flow. *Computational Geosciences* **12**: 451–472.

D'Haese CMF, Putti M, Paniconi C, Verhoest NEC. 2007. Assessment of adaptive and heuristic time stepping for variably saturated flow. *International Journal for Numerical Methods in Fluids* **53**: 1173–1193.

Discacciati M, Miglio E, Quarteroni A. 2002. Mathematical and numerical models for coupling surface and groundwater flows. *Applied Numerical Mathematics* **43**: 57–74, DOI: 10·1016/S0168-9274(02)00125-3.

Ebel BA. 2007. *Process-based characterization of near-surface hydrologic response and hydrologically driven slope instability*. PhD Dissertation, Department of Geological and Environmental Sciences, Stanford University, Stanford.

Ebel BA, Loague K. 2006. Physics-based hydrologic-response simulation: Seeing through the fog of equifinality. *Hydrological Processes* **20**: 2887–2900. DOI: 10·1002/hyp.6388.

Ebel BA, Loague K. 2008. Rapid simulated hydrologic response within the variably saturated near surface. *Hydrological Processes* **22**: 464–471, DOI: 10·1002/hyp.6926.

Ebel BA, Loague K, Montgomery DR, Dietrich WE. 2008. Physics-Based Continuous Simulation of Long-Term Near-Surface Hydrologic Response for the Coos Bay Experimental Catchment. *Water Resources Research* **44**: W07417, DOI:10·1029/2007WR006442.

Ebel BA, Loague K, VanderKwaak JE, Dietrich WE, Montgomery DR, Torres R, Anderson SP. 2007. Near-surface hydrologic response for a steep, unchanneled catchment near Coos Bay, Oregon: 2. Physics-based simulations. *American Journal of Science* **307**: 709–748, DOI:10·2475/04·2007·03.

Fairbanks J, Panday S, Huyakorn P. 2001. Comparisons of linked and fully coupled approaches to simulating conjunctive surface/subsurface flow and their interactions. In *MODFLOW 2001 and Other Modeling Odysseys, Conference Proceedings*, Seo B, Poeter E, Zheng C (eds). Golden, CO; 356–361.

Freeze RA. 1972a. Role of subsurface flow in generating runoff 1. Base flow contributions to channel flow. *Water Resources Research* **8**: 609–624.

Freeze RA. 1972b. Role of subsurface flow in generating runoff 2. Upstream source areas. *Water Resources Research* **8**: 1272–1283.

Furman A. 2008. Modeling coupled surface-subsurface flow processes: a review. *Vadose Zone Journal* **7**: 741–756, DOI: 10·2136/vzj2007·0065.

Gartling D, Hickox C, Givler R. 1996. Simulation of coupled viscous and porous flow Problems. *Computational Fluid Dynamics* **7**: 23–48.

Gerke HH, van Genuchten MTh. 1993a. A dual-porosity model for simulating the preferential movement of water and solutes in structured porous media. *Water Resources Research* **29**: 305–319.

Gerke HH, van Genuchten MTh. 1993b. Evaluation of a first-order water transfer term for variably-saturated dual-porosity models. *Water Resources Research* **29**: 1225–1238.

Gerke HH, van Genuchten MTh. 1996. Macroscopic representation of structural geometry for simulating water and solute movement in dual-porosity media. *Advances in Water Resources* **19**: 343–357.

Gunduz O, Aral MM. 2003. Simultaneous solution of coupled surface water/groundwater flow systems. In *International Conference on River Basin Management*, Brebbia CA (ed). Gran Canaria Islands; 25–34.

Gunduz O, Aral MM. 2005. River networks and groundwater flow: a simultaneous solution of a coupled system. *Journal of Hydrology* **301**: 216–234.

Hallett PD, Nunan N, Douglas JT, Young IM. 2004. Millimeter-scale spatial variability in soil water sorptivity: scale, surface elevation, and subcritical repellency effects. *Soil Science Society of America journal* **68**: 352–358.

Hammond GE, Valocchi AJ, Lichtner PC. 2005. Application of Jacobian-free Newton- Krylov with physics-based preconditioning to biogeochemical transport. *Advances in Water Resources* **28**: 359–376, DOI:10·1016/j.advwatres.2004·12·001.

Heppner CS. 2007. *A dam problem: characterizing the upstream hydrologic and geomorphologic impacts of dams*. PhD Dissertation, Department of Geologicaland Environmental Sciences, Stanford University, Stanford.

Heppner CS, Loague K. 2008. A dam problem: simulated upstream impacts for the Searsville Watershed. *Ecohydrology* **1**: 408–424.

Heppner CS, Loague K, VanderKwaak JE. 2007. Long-term InHM simulations of hydrologic response and sediment transport for the R-5 catchment. *Earth Surface Processes and Landforms* **32**: 1273–1292, DOI: 10·1002/esp.1474.

Heppner CS, Ran Q, VanderKwaak JE, Loague K. 2006. Adding sediment transport tothe Integrated Hydrology Model (InHM): development and testing. *Advances in Water Resources* **9**: 930–943, DOI:10·1016/j.advwatres.2005·08·003.

Herbst M, Gottschalk S, Reißel M, Hardelauf H, Kasteel R, Javaux M, Vanderborght J, Vereecken H. 2008. On preconditioning for a parallel solution of the Richards equation. *Computational Geosciences* **34**: 958–1963, DOI:10·1016/j.cageo.2008·02·020.

Hromadka TV, Berenbrock CE, Freckleton JR, Guymon GL. 1985. A two-dimensional dam-break flood plain model. *Advances in Water Resources* **8**: 7–14.

Hunt RJ, Prudic DE, Walker JF, Anderson MP. 2008. Importance of unsaturated zone flow for simulating recharge in a humid climate. *Ground Water* **46**: 551–560.

Jarvis NJ, Jansson PE, Dik PE, Messing I. 1991. Modelling water and solute transport in macroporous soil: 1. Model description and sensitivity analysis. *Journal of Soil Science* **42**: 59–70.

Jones JP, Sudicky EA, Brookfield AE, Park Y-J. 2006. An assessment of the tracer-based approach to quantifying groundwater contributions to streamflow. *Water Resources Research* **42**: W02407, DOI:10·1029/2005WR004130.

Jones JP, Sudicky EA, McLaren RG. 2008. Application of a fully-integrated surface-subsurface flow model at the watershed-scale: a case study. *Water Resources Research* **44**: W03407, DOI:10·1029/2006WR005603.

Jones JE, Woodward CS. 2001. Newton-Krylov-multigrid solvers for large-scale, highly heterogeneous, variably saturated flow problems. *Advances in Water Resources* **24**: 763–774, DOI: 10·1016/S0309-1708(00)00075-0.

Knoll DA, Keyes DE. 2004. Jacobian-free Newton-Krylov methods: a survey of approaches and applications. *Journal of Computational Physics* **193**: 357–397.

Kollet SJ, Maxwell RM. 2006. Integrated surface- groundwater flow modeling: A free-surface overland flow boundary condition in a parallel groundwater flow model. *Advances in Water Resources* **29**: 945–958, DOI:10·1016/j.advwatres.2005·08·006.

Kollet SJ, Maxwell RM. 2008a. Capturing the influence of groundwater dynamics on land surface processes using an integrated, distributed watershed model. *Water Resources Research* **44**: W02402, DOI:10·1029/2007WR006004.

Kollet SJ, Maxwell RM. 2008b. Demonstrating fractal scaling of baseflow residence time distributions using a fully-coupled groundwater and land surface model. *Geophysical Research Letters* **35**: L07402, DOI:10·1029/2008GL033215.

Kollet SJ, Zlontik VA. 2003. Stream depletion predictions using pumping test data from a heterogeneous stream-aquifer system (a case study from the Great Plains, USA). *Journal of Hydrology* **281**: 96–114.

Kropinski MCA. 1990. *Numerical techniques for saturated-unsaturated flow*. M.Sc. thesis, Department of Applied Mathematics, University of Waterloo, Ontario, Canada.

Lamberti P, Pilati S. 1996. Flood propagation models for real-time forecasting. *Journal of Hydrology* **175**: 239–265.

Langevin C, Swain E, Wolfert M. 2005. Simulation of integrated surface water-groundwater flow and salinity for a coastal wetland and adjacent estuary. *Journal of Hydrology* **314**: 212–234.

Lemieux J-M, Sudicky EA, Peltier WR, Tarasov L. 2008. Dynamics of groundwater recharge and seepage over the Canadian landscape during the Wisconsinian glaciation. *Journal of Geophysical Research* **113**: F01011, DOI: 10·1029/2007JF000838.

Li Q, Unger AJA, Sudicky EA, Kassenaar D, Wexler EJ, Shikaze S. 2008. Simulating the multi-seasonal response of a large-scale watershed with a 3D physically-based hydrologic model. *Journal of Hydrology* **357**: 317–336, DOI: 10·1016/j.jhydrol.2008·05·024.

Lighthill MJ, Whitham GB. 1955. On kinematic waves. I. Flood movement in long rivers. *Proceedings of the Royal Society of London. Series A, Mathematical and Physical Sciences* **229**: 281–316, DOI: 10·1098/rspa.1955·0088.

Loague K. 1990. R-5 revisited: 2. Re-evaluation of a quasi-physically based rainfall-runoff model with supplemental information. *Water Resources Research* **26**: 973–987.

Loague K, Corwin DL. 2007. Scale issues. In *The Handbook of Groundwater Engineering*, Delleur JW (ed.). CRC Press; 25·1–25·21.

Loague KM, Freeze RA. 1985. A comparison of rainfall-runoff modeling techniques on small upland catchments. *Water Resources Research* **21**: 229–248.

Loague K, Heppner CS, Abrams RH, VanderKwaak JE, Carr AE, Ebel BA. 2005. Further testing of the Integrated Hydrology Model (InHM) with event data from the R-5 catchment. *Hydrological Processes* **19**: 1373–1398, DOI:10·1002/hyp.5566.

Loague K, Heppner CS, Mirus BB, Ebel BA, Ran Q, Carr AE, BeVille SH, VanderKwaak JE. 2006. Physics-based hydrologic-response simulation: foundation for hydroecology and hydrogeomorphology. *Hydrological Processes* **20**: 1231–1237.

Loague K, Kyriakidis PC. 1997. Spatial and temporal variability in the R-5 infiltration data set: Deja vu and rainfall-runoff simulations. *Water Resources Research* **33**: 2883–2895.

Loague K, VanderKwaak JE. 2002. Simulating hydrologic-response for the R-5 catchment: Comparison of two models and the impact of the roads. *Hydrological Processes* **16**: 1015–1032, DOI:10·1002/hyp.316.

Loague K, VanderKwaak JE. 2004. Physics-based hydrologic response simulation: Platinum bridge, 1958 Edsel, or useful tool. *Hydrological Processes* **18**: 2949–2956, DOI:10·1002/hyp.5737.

Markstrom SL, Niswonger RG, Regan RS, Prudic DE, Barlow PM. 2008. *GSFLOW-Coupled Ground-water and Surface-water FLOW model based on the integration of the Precipitation-Runoff Modeling System (PRMS) and the Modular Ground-Water Flow Model (MODFLOW-2005)*, U.S. Geological Survey Techniques and Methods 6-D1; 240.

Maxwell RM, Chow FK, Kollet SJ. 2007. The groundwater- land-surface- atmosphere connection: soil moisture effects on the atmospheric boundary layer in fully-coupled simulations. *Advances in Water Resources* **30**: 2447–2466, DOI:10·1016/j.advwatres.2007·05·018.

Maxwell RM, Kollet SJ. 2008a. Quantifying the effects of three-dimensional subsurface heterogeneity on Hortonian runoff processes using a coupled numerical, stochastic approach. *Advances in Water Resources* **31**: 807–817, DOI:10·1016/j.advwatres.2008·01·020.

Maxwell RM, Kollet SJ. 2008b. Interdependence of groundwater dynamics and land-energy feedbacks under climate change. *Nature Geoscience* **1**: 665–669, DOI:10·1038/ngeo315.

Maxwell RM, Miller NL. 2005. Development of a coupled land surface and groundwater model. *Journal of Hydrometeorology* **6**: 233–247, DOI: 10·1175/JHM422·1.

McLaren RG, Forsyth PA, Sudicky EA, VanderKwaak JE, Schwartz FW, Kessler JH. 2000. Flow and transport in fractured tuff at Yucca Mountain: numerical experiments on fast preferential flow mechanisms. *Journal of Contaminant Hydrology* **43**: 211–238, DOI:10·1016/S0169-7722(00)00085-1.

Mills AJ, Feya MV. 2004. Frequent fires intensify soil crusting: physicochemical feedback in the pedoderm of long-term burn experiments in South Africa. *Geoderma* **121**: 45–64.

Mirus BB, Ebel BA, Loague K, Wemple BC. 2007. Simulated effect of a forest road on near-surface hydrologic response: redux. *Earth Surface Processes and Landforms* **32**: 126–142, DOI: 10·1002/esp.1387.

Mirus BB, Loague K, VanderKwaak JE, Kampf SK, Burges SJ. 2009. A hypothetical reality of Tarrawarra-like hydrologic response. *Hydrological Processes* **23**: 1093–1103, DOI: 10.1002/hyp.7241.

Morita M, Yen B-C. 2000. Numerical methods for conjunctive two-dimensional surface and three-dimensional sub-surface flows. *International Journal for Numerical Methods in Fluids* **32**: 921–957.

Morita M, Yen B-C. 2002. Modeling of conjunctive two-dimensional surface-three-dimensional subsurface flows. *Journal of Hydraulic Engineering-ASCE* **128**: 184–200.

Mualem Y, Assouline S, Rohdenburg RH. 1990. Rainfall induced soil seal (A). A critical review of observations and models. *Catena* **17**: 185–203.

Noto LV, Ivanov VY, Bras RL, Vivoni ER. 2008. Effects of Initialization on Response of a Fully-Distributed Hydrologic Model. *Journal of Hydrology* **352**: 107–125.

Panday S, Huyakorn PS. 2004. A fully coupled physically-based spatially-distributed model for evaluating surface/subsurface flow. *Advances in Water Resources* **27**: 360–382.

Park Y-J, Sudicky EA, Panday S, Sykes JF, Guvanasen V. 2008. Application of implicit sub-time stepping to simulate flow and transport in fractured porous media. *Advances in Water Resources* **31**: 995–1003.

Perkins SP, Koussis AD. 1996. Stream aquifer interaction model with diffusive wave routing. *Journal of Hydraulic Engineering-ASCE* **122**: 210–218, DOI 10·1061/(ASCE)0733–9429(1996)122 : 4(210).

Peyrard D, Sauvage S, Vervier P, Sanchez-Perez JM, Quintard M. 2008. A coupled vertically integrated model to describe lateral exchanges between surface and subsurface in large alluvial floodplains with a fully penetrating river. *Hydrological Processes* **22**: 4257–4273, DOI:10·1002/hyp.7035.

Philip JR. 1957. The theory of infiltration, 4, Sorptivity and algebraic infiltration equations. *Soil science* **84**: 257–264.

Qu Y, Duffy CJ. 2007. A semidiscrete finite volume formulation for multiprocess watershed simulation. *Water Resources Research* **43**: W08419.

Ran Q. 2006. *Regional scale landscape evolution: Physics-based simulation of hydrologically-driven surface erosion*. PhD Dissertation, Department of Geological and Environmental Sciences, Stanford University, Stanford.

Ran Q, Heppner CH, VanderKwaak JE, Loague K. 2007. Further testing of the Integrated Hydrology Model (InHM): Multiple-species sediment transport. *Hydrological Processes* **21**: 1522–1531, DOI: 10·1002/hyp.6642.

Refsgaard J, Storm B. 1996. MIKE SHE. In *Computer Models of Watershed Hydrology*. Water Resources Publications: Fort Collins.

Richardson CP, Parr AD. 1991. Friction and free-surface flow over porous media. *Journal of Hydraulic Engineering-ASCE* **117**: 1496–1512.

Roberts RJ, Clanton CJ. 2000. Surface seal hydraulic conductivity as affected by livestock manure application. *Transactions of the ASAE* **43**: 603–613.

Robinson DA, Phillips CP. 2001. Crust development in relation to vegetation and agricultural practice on erosion susceptible, dispersive clay soils from central and Southern Italy. *Soil and Tillage Research* **60**: 1–9.

Römkens MJM, Prasad SN, Parlange J-Y. 1990. *Surface seal development in relation to rainstorm intensity. Catena Supplement No. 17, Catena*, Verlag, Germany, 1–11.

Salinger A, Aris R, Derby I. 1994. Finite element formulations for large-scale, coupled flows in adjacent porous and open fluid domains. *International Journal for Numerical Methods in Fluids* **18**: 1185–1209.

Schoups G, Hopmans JW, Young CA, Vrugt JA, Wallender WW, Tanji KK, Panday S. 2005. Sustainability of irrigated agriculture in the San Joaquin Valley, California. *Proceedings of the National Academy of Sciences USA* **102**: 15352–15356, DOI: 10·1073/pnas.0507723102.

Siegrist RL. 1987. Soil clogging during subsurface wastewater infiltration as affected by effluent composition and loading rate. *Journal of Environmental Quality* **16**: 181–187.

Smerdon BD, Medoza CA, Devito KJ. 2007. Simulations of fully coupled lake groundwater exchange in a subhumid climate with an integrated hydrologic model. *Water Resources Research* **43**: W01416, DOI: 10·1029/2006WR005137.

Smerdon BD, Mendoza CA, Devito KJ. 2008. Influence of subhumid climate and water table depth on groundwater recharge in shallow outwash aquifers. *Water Resources Research* **44**: W08427, DOI:10·1029/2007WR005950.

Smith RE, Hebbert RHB. 1983. Mathematical simulation of interdependent surface and subsurface hydrologic processes. *Water Resources Research* **19**: 987–1001.

Smith RE, Woolhiser DA. 1971. Overland flow on an infiltrating surface. *Water Resources Research* **7**: 899–913.

Sudicky EA. 1990. The Laplace transform Galerkin technique for efficient time-continuous solution of solute transport in double-porosity media. *Geoderma* **46**: 209–232.

Sudicky EA, Jones JP, Park Y-J, Brookfield AE, Colautti D. 2008. Simulating complex flow and transport dynamics in an integrated surface-subsurface modeling framework. *Geosciences Journal* **12**: 107–122, DOI: 10·1007/s12303-008-0013-x.

Sudicky EA, Therrien R, Park Y-J, McLaren RG, Jones JP, Lemieux J-M, Brookfield AE, Colautti D, Panday S. 2005. On the challenge of integrated surface-subsurface flow and transport modeling at multiple catchment scales. *Geological Society of America Abstracts with Programs* **37**(7): 28, 2005 Salt Lake City Annual Meeting.

Sulis M, Kollet SJ, Maxwell RM, Paniconi C, Putti M, AGU. 2006. Comparison of two approaches for resolving the coupling term in groundwater-surface water hydrological models. Abstract H31H-05. *EOS Transactions* **87**(52): Fall Meeting Supplement.

Talsma T. 1969. In situ measurement of sorptivity. *Australian Journal of Soil Research* **7**(3): 269–276.

Therrien R, Sudicky EA. 1996. Three-dimensional analysis of variably-saturated flow and transport in discretely fractured porous media. *Journal of Contaminant Hydrology* **23**: 1–44.

Therrien R, McLaren RG, Sudicky EA, Panday SM. 2005. *HydroGeoSphere: A Three-Dimensional Numerical Model Describing Fully-Integrated Subsurface and Surface Flow and Solute Transport*. Groundwater Simulations Group, University of Waterloo: Waterloo, 322.

Todini E, Bossi A. 1987. PAB (Parabolic and Backwater), an unconditionally stable flood routing scheme particularly suited for real time forecasting and control. *Journal of Hydraulic Research* **25**: 405–424.

VanderKwaak JE. 1999. *Numerical simulation of flow and chemical transport in integrated surface-subsurface hydrologic systems*. PhD Dissertation, University of Waterloo, Waterloo, 217.

VanderKwaak JE, Loague K. 2001. Hydrologic-response simulations for the R-5 catchment with a comprehensive physics-based model. *Water Resources Research* **37**: 999–1013.

VanderKwaak JE, Sudicky EA. 2000. Application of a physically-based numerical model of surface and subsurface water flow and solute transport. In *Calibration and Reliability in Groundwater Modelling*, *IAHS Publication No. 265*, ModelCARE 99. IAHS: Zürich; 515–523.

van Genuchten MTh, Wierenga PJ. 1976. Mass transfer studies in sorbing porous media: analytical solution. *Soil Science Society of America Journal* **40**: 473–480.

van Genuchten MTh, Dalton FN. 1986. Models for simulating salt movement in aggregated field soils. *Geoderma* **38**: 165–183.

Warren JE, Root PJ. 1963. The behavior of naturally fractured reservoirs. *Society of Petroleum Engineers Journal* **228**: 245–255.

Weng Ph, Giraud F, Fleury P, Chevallier C. 2003. Characterising and modeling groundwater discharge in an agricultural wetland on the French Atlantic coast. *Hydrology and Earth System Sciences* **7**: 33–42.

Wood EF, Sivapalan M, Beven K, Band L. 1988. Effects of Spatial Variability and Scale with Implications to Hydrologic Modeling. *Journal of Hydrology* **102**: 29–47.

Yeh GT, Huang G, Cheng HP, Zhang F, Lin HC, Edris E, Richards D. 2005. A First principle, physics based watershed model: WASH123D. In *Watershed Models*, Singh VP, Frevert DK (eds). CRC Press LLC: Boca Raton; 211–244.

Yen BC, Tsai CW-S. 2001. On noninertia wave versus diffusion wave in flood routing. *Journal of Hydrology* **244**: 97–104.

Zehe E, Blöschl G. 2004. Predictability of hydrologic response at the plot and catchment scales: Role of initial conditions. *Water Resources Research* **40**: W10202, DOI:10·1029/2003WR002869.